OPTIMIZING OF THE DEGREE OF ELONGATION IN A SINGLE PASS DURING HOT BARS ROLLING IN THE OVAL-ROUND ROLL PASS SCHEDULE

HÁBA Jan, FABÍK Richard

[1]*VSB - Technical University of Ostrava, Faculty of Metallurgy and Materials Engineering, Ostrava, Czech Republic, EU, richard.fabik@vsb.cz,*

Abstract

The main disadvantage of using classical (butt) oval roll groove in the oval-round roll pass schedule is the relatively small coefficient of elongation. This fact requires a larger number of passes to achieve the final dimension of the bar (or wire). This may be a problem for a rolling mill with fewer stands. The coefficient of elongation can be increased by reducing the distance between the rolls. However, we are facing problems with the arising of the flash in the second (round) groove. A possible solution is to use an elliptical oval groove in the first pass which causes greater elongation in the round groove. This paper deals with the computer simulation of hot bars rolling in two consecutive passes in the oval-round roll pass schedule by FORGE. The initial and boundary conditions of the FE analysis was validated and verified by a laboratory hot rolling of round steel bars on flat and round grooved rolls at different rolling temperatures. We compared the rolling forces and the rolled shapes after the individual passes. In this paper the different settings of butt and elliptical ovals and their impact on the overall coefficient of elongation in both passes are presented. Our results showed that the use of an elliptical groove can greatly improve the overall coefficient of elongation.

Keywords: Hot bars rolling, roll pass schedule, FE analysis, coefficient of elongation

1. INTRODUCTION

The main object of metallurgical research and development in the field of the rolling of long product is to optimise the means of production for the manufacturing of a rolled product. The optimisation criteria may vary, depending on the requirements for the final product. In general, they should be based on a full understanding of the manufacturing process. In hot rolling processes, the knowledge of deformation mechanisms is crucial. Without knowing the impact of friction, material properties and tool geometry on the operation of the process, it is impossible to propose optimum shapes of grooves and the configuration of working rolls. Field (pilot) rolling at e.g. a bar rolling mill is too expensive, insufficiently flexible and it is often difficult to get all process parameters under complete control (dimensions of billets, rolls and grooves, setting guides, roll speeds, the presence of draws and loops between stands, etc.). Laboratory modelling on plastometers is considered more of an additional experiment, for a description of the process of deformation of roll stocks during hot rolling, for setting certain material characteristics (typically, for example, relation of yield strength on temperature, strain and strain rate). Laboratory modelling on laboratory roll stands requires providing identical geometry to actual rolling, which is often practically impossible. Nonetheless, this equipment can at least be used for the verification of boundary conditions of FE analysis under similar conditions as presented in our paper). This is why process modelling using computer simulation has an increasing importance in today's hot rolling processes [1-14].

2. DESCRIPTION OF EXPERIMENT

2.1. Determining boundary conditions of FE analysis using laboratory rolling

The assignment was to perform laboratory-condition hot rolling of round-section bars from AISI 304 steel on a laboratory two-high roughing reverse stand [9] with roll diameter (in the main section) of 350 mm.

The result of the work are records of measures values during rolling (especially time, temperature, rolling force and torque) and graphic data of the cross-section shape of respective roll stocks, which were subsequently compared to results of a finite element (FE) analysis performed using the FORGE software. Rolling of the initial billet (diameter 42 mm) was performed on the flat roll section with a nominal roll gap of 20 mm, which simulated rolling in an oval groove and subsequently the stock was rolled in a round groove to a diameter of 33.6 mm. Temperatures of 1100 and 1200 °C were tested.

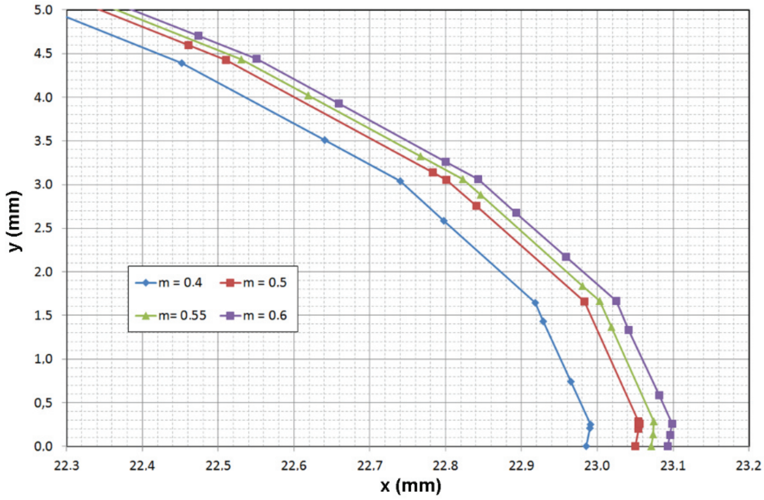

Figure 1 Effect of friction factor *m* on the shape of the cross-section of the stock 30 mm behind the input plane during rolling on a wane (T = 1200 °C)

The actual FE analysis of the laboratory rolling was performed for various friction factor values and various finite element mesh sizes. The graph illustrating the effect of the friction factor on the shape of the roll stock after the first pass in the roll stock at 1200 °C is shown in **Figure 1**. Based on the shape best corresponding to the result of laboratory rolling, a friction factor of m = 0.6 was selected for further simulations.

2.2. Optimization of rolling bars in an oval-round roll pass schedule

The original aim of our simulations was to determine the energy-force rolling parameters according to the provided pass schedule for a new rolling mill. However, we very soon experienced problems with the roll pass design, particularly with an insufficient elongation coefficient in the pair of oval-round grooves. Preparation of the roll pass schedule is foremost limited to the number of stands of the mill; if the elongation coefficient has too small of a reduction in the individual passes it is impossible to achieve the required final rod dimensions.

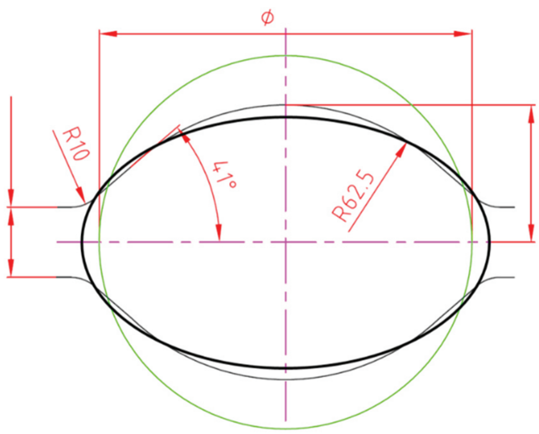

Figure 2 Comparison of original blunt oval (thin black line) with the new elliptical oval (bold black line)

Besides the simulation of the provided roll pass design, we had to prepare our own roll pass design, initially by modifying the setting of the partial reductions while maintaining the shape of the grooves, and subsequently also by replacing the blunt oval with an elliptical oval. The difference between a blunt and elliptical oval is best shown in **Figure 2** where the elliptical oval is plotted in black over the current calibre. The aim is to get more material away from the central section in the oval grooves and thereby to support the elongation in the subsequent round grooves.

An overview of the setting of individual grooves setting variants is shown in **Table 1**. The basic simulation parameters and boundary and initial conditions are provided in **Table 2.** Yield strength was determined using the Spittel equation from the FORGE database:

$$\sigma_f = Ae^{m_1 T}\varepsilon^{m_2} e^{\frac{m_4}{\varepsilon}} \dot{\varepsilon}^{m_3} \quad (1)$$

where T is temperature (°C), ε is strain; $\dot{\varepsilon}$ is strain rate (1/s), m_1= -0.00364; m_2 = 0.00037; m_3 = 0.10489; m_4 = -0.04223

Table 1 Variants

	Variant	Rolls shift *dx* (mm)
blunt oval	BV01	0.0
	BV02	-0.5
	BV03	-1.0
	BV04	-1.5
	BV05	-2.0
Elliptical oval	Variant	Dimension of ellipse (mm)
	EV01	57/32
	EV02	57/33
	EV03	58/32
	EV04	58/33
	EV05	58/34

Table 2 Setting simulation and initial and boundary conditions

Stand	1	2	3
Main dimension			
Starting cross-section	d = 42	Result from previous pass	
Rolls diameter [m]	0.276	0.276	0.276
Boundary conditions		**Initial condition**	
Friction	0.6	Billet temperature	1200 °C
Rolls velocity (rpm)	12.33	Tools temperature	100 °C
Pusher velocity (m/s)	220	Ambient temperature	20 °C
Heat transfer Billet -> cylinder (W.m^{-2}.K^{-1})	10 000	**Set up**	
		Axis of symmetry	*x, y*
Heat transfer	air computation, ε = 0.88	Plane of symmetry	(1 0 1) a (1 1 0)
		FEM formulation	rigid-plastic

3. DISCUSSION OF RESULTS

3.1. Basic simulation BV01

The development of the shape of the roll stock in the first three monitored passes is documented in **Figure 3**, and **Table 3** shows the values of the cross-section of the roll stock and cumulated elongation coefficient. The main problem is insufficient elongation in the oval grooves which causes the overfilling of the 1st grooves and subsequently the formation of an inconsiderable flash in the second (round) grooves. Thereafter, the situation continues to worsen; though an overlay or other defect isn't formed yet, but the third calibre is overfilled even more than the first, so the situation will continue to deteriorate.

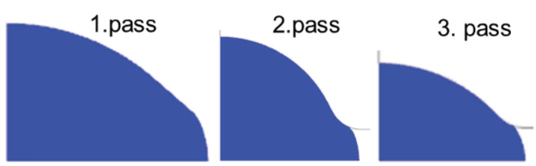

Figure 3 Shape of ¼ section of roll stock in the output rolling plane for respective passes (variant BV01)

3.2. Modification of basic simulation by a change of the distance between rollers (BV02 to BV05)

As can be seen in **Table 3** for variant BV02 to BV05, the increase in reduction in the first pass leads to an increase in the coefficient of elongation after the 1st pass; the cumulated coefficient of elongation after the 2nd pass is also bigger, but the difference is not substantial. Moreover, with the increase of the reduction in the first pass leads to an increasing overfilling of the first oval calibre. The situation for the BV05 variant is documented in **Figure 4**. At the cost of overfilling the 1st calibre, the required cross-section area of the roll stock was achieved in the subsequent passes. Nonetheless, this variant is quite dangerous due to the risk of formation of a overlap in the second pass if the input billet area should slightly increase.

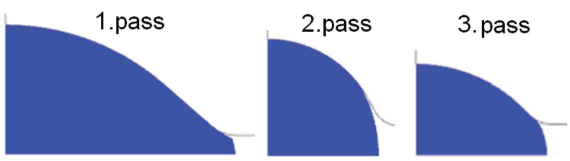

Figure 4 Shape of ¼ section of roll stock in the output rolling plane for respective passes (variant BV05)

Table 3 Cross-section area of the roll stock for individual passes and coefficient of elongation for all rolling variants

	Stand 1					Stand 2			Stand 3	
	Variant	**Rolls shift** ***dx*** **(mm)**	**Cross section area** ***A*** **(mm²)**	**Coeff. of elongation** ***λ*** **(-)**		**Cross section area** ***A*** **(mm²)**	**cumulated** ***λ*** **(-)**		**Cross section area** ***A*** **(mm²)**	**cumulated** ***λ*** **(-)**
blunt oval	BV01	0.0	1087	1.26	→	835	1.64	→	633	2.16
	BV02	-0.5	1048	1.31	→	824	1.68			
	BV03	-1.0	1008	1.36	→	811	1.70			
	BV04	-1.5	965	1.42	→	797	1.73			
	BV05	-2.0	920	1.48	→	779	1.78	→	618	2.24
Elliptical oval		**Dimension of ellipse (mm)**	**Cross section area** ***A*** **(mm²)**	**Coeff. of elongation** ***λ*** **(-)**		**Cross section area** ***A*** **(mm²)**	**Total** ***λ*** **(-)**		**Cross section area** ***A*** **(mm²)**	**Total** ***λ*** **(-)**
	EV01	57/32	1055	1.42	→	774	1.79	→	620	2.24
	EV02	57/33	1080	1.34	→	787	1.76			
	EV03	58/32	1065	1.37	→	777	1.78			
	EV04	58/33	1052	1.33	→	789	1.74			
	EV05	58/34	1163	1.31	→	809	1.70			

3.3. Use of elliptical oval (EV01 to EV05)

The basic parameters of the elliptical oval and the corresponding results of the cross-section area and cumulated coefficient of elongation are also shown in **Table 3**. The results confirmed out presumptions that even though the coefficient of elongation in the 1st calibre was similar to the value for the blunt oval, due to the better shape the 2nd pass led to elongation comparable to the BV05 variant but without the need to overfill the first calibre, as is documented in **Figure 5**.

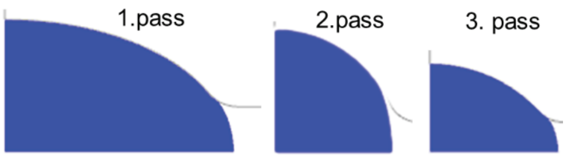

Figure 5 Shape of ¼ section of roll stock in the output rolling plane for respective passes (variant EV01)

A general comparison of the roll stock shape and deformation intensity field after the 1st pass for the basic variant (BV01), for the best variant achieved by the setting of rollers (BV05), and for the best variant achieved by using an elliptical oval (EV01) is shown in **Figure 6**. The diagram clearly shows that using the elliptical oval leads to a more uniform strain field in the roll stock.

In **Figure 7** we can see the result for the same set of variants, but this time after the 2nd pass. The shape of the roll stock for variants BV05 and EV01 is almost identical, but there is a very interesting difference in the equivalent strain field, which is more uniform for variant EV01 and also 1.8 times larger, which has a positive side-effect on the microstructure of the roll stock.

The disadvantage of using an elliptical oval is greater energy-force demands of rolling in a round calibre, as is shown in **Table 4**.

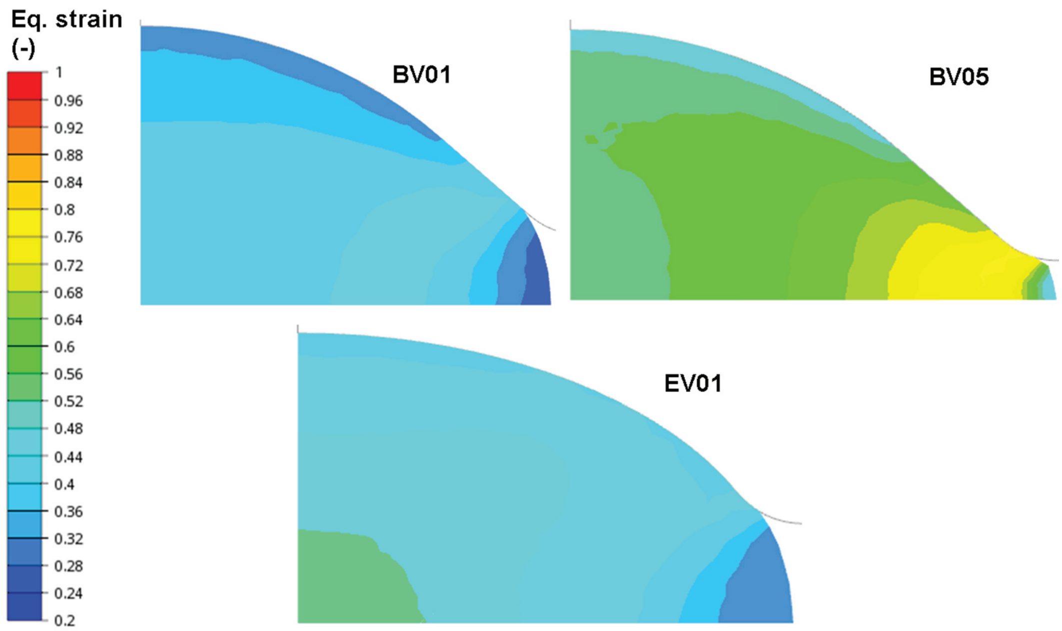

Figure 6 Shape of ¼ section of roll stock and equivalent strain field in the output rolling plane after the first pass for the selected simulation variants

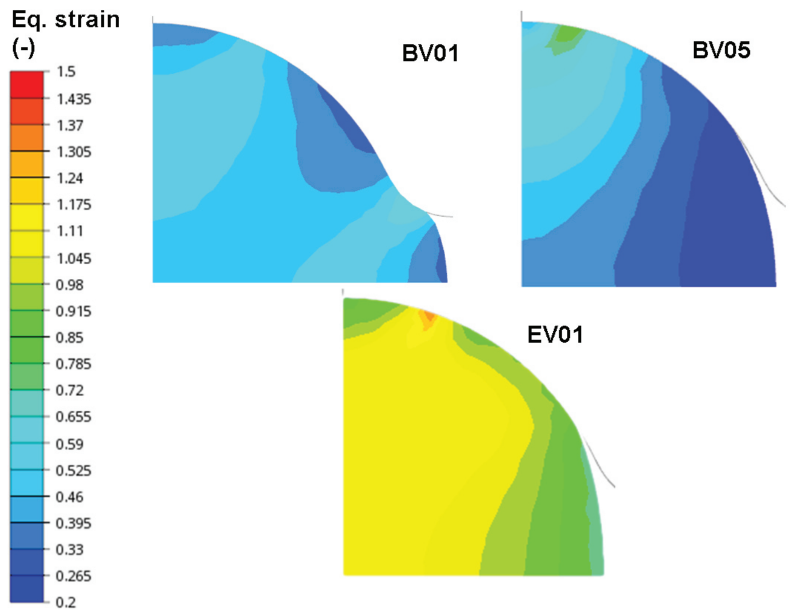

Figure 7 Shape of ¼ section of roll stock and equivalent strain field in the output rolling plane after the second pass for the selected simulation variants

Table 4 Energy-force parameters of rolling for the analysed variants

	Stand 1		Stand 2	
Variant	**Rolling Force (kN)**	**Rolling Torque (Nm)**	**Rolling Force (kN)**	**Rolling Torque (Nm)**
BV01	68.9	1183	40.9	832
BV05	105.6	1989	61.9	1171
EV01	95.2	1840	60.8	1438

4. CONCLUSIONS

The demonstrated simulations showed that programs based on FEM can be used for the optimization of pass schedules for rolling long stock. In this case it proved to be advantageous to use an oval grooves of a different design (elliptical) to provide for the required coefficient of elongation without risking the overfilling of the oval grooves. As yet, our results were not executed directly at a rolling mill, so operational validation is still to be done.

Another possible option to explore in the field of optimization of pass schedules for rolling round bars is to replace non-finishing round grooves with opsetting oval grovess (the shape of the calibre is similar to an egg shape). Mathematical modelling based on FEM can also be applied very successfully in this case.

ACKNOWLEDGEMENTS

The research was supported by the grant project LO1203 (MŠMT ČR).

REFERENCES

[1] GLOWACKI, M., The mathematical modelling of thermo-mechanical processing of steel during multi-pass shape rolling, *Journal of Materials Processing Technology*, Vol. 168, No 2, 2005, pp. 336-343

[2] LEE, S., CHOI, J., Deformation analysis of surface defect on hot rolling by 3-D FEM simulation, *Revue de Métallurgie*, **Vol.** 3, March 2008, pp. 127-135

[3] FABÍK, R., AKSENOV, S. Optimization of crop losses by finite element simulation of slab edging. Metal Forming Conference 2008, *Steel research int.*, 2008, 79 Special Edition, No. 1, pp. 432-439.

[4] GLOWACKI M., KUZIAK, R., MALINOVSKI, Z., M. PIETRZYK, M., Modelling of heat transfer, plastic flow and microstructural evolution during shape rolling, *JOMPT*, Volume 53, no 1-2, August 1995, pp. 159-166

[5] LENARD,J.G., PIETRZYK, M., CSER, Y.: Mathematical and Physical Simulation of the Properties of Hot Rolled Products, Elsevier Science Ltd., 1999, ISBN-0080427014

[6] AKSENOV S., KLIBER J., CHUMACHENKO E., Comparison of 3D and 2.5D finite element simulation principles for rolling in grooves modeling. In Computer methods in materials science, Vol.7, 2007, pp.191-195

[7] CHUNG W.K., CHOI S.K., THOMSON P.F., Three-dimensional simulation of the edge rolling process by the explicit finite-element method, *JOMPT*, vol. 38, 1993, pp. 85-102.

[8] GRATACOS P., COUPU J., 3D finite element code application in hot rolling, *La Revue deMetallurgie* - CIT 91, vol. 11, 1994, pp. 1672-1679, (in French).

[9] XIONG S.W., LIU X.H., WANG G.D., ZHANG Q., Simulation of veritical-horizontal rolling process during width reduction by full 3D rigid-plastic FEM. *JMEP*, vol. 6, 1997, pp. 757-765.

[10] XIONG S.W., LIU X.H., WANG G.D., ZHANG Q., Simulation of slab edging by the 3-D rigid-plastic FEM., *JOMPT*, vol. 69, 1997, pp. 37-44.

[11] XIONG S.W., LIU X.H., WANG G.D., ZHANG Q., A three-dimensional finite element simulation of the vertical-horizontal rolling process in the width reduction of slab. *JOMPT*, vol. 101, 2000, pp. 146-151.

[12] XIONG S.W, ZHENG G., LIU X., WANG G., Analysis of the non-steady state vertical-horizintal rolling process in roughing trains by the three-dimensional FEM. *JOMPT*, vol. 120, 2002, pp. 53-61

[13] JIANG Z.Y., TIEU A.K., LU C., Mechanical modeling of friction variation in slab edging with a FEM approach. *Trib. Int.* vol. 37, 2004, pp. 733-742

[14] FABÍK, R., KLIBER, J., MAMUZIĆ, I., KUBINA, T., AKSENOV, S. Mathematical modelling of flat and long hot rolling based on finite element methods (FEM). *Metalurgija = Metallurgy*, 2012, Vol. **51,** no **3,** pp. **341-344**.

[15] SCHINDLER, I., HADASIK, E., KOPEČEK, J., KAWULOK, P., FABÍK, R., OPĚLA, P., RUSZ, S., KAWULOK, R., JABLOŃSKA, M. Optimization of laboratory hot rolling of brittle Fe-40at.%Al-Zr-B aluminide. *Archives of metallurgy and materials*, 2015, Vol. 60, no. 3, pp. 1693-1701.